American Journal of Engineering Research (AJER)
e-ISSN: 2320-0847 p-ISSN : 2320-0936
Volume-4, Issue-11, pp-01-07
www.ajer.org
Research Paper Open Access

# Design Analysis of a Locally Fabricated Palm Kernel Shells Grinding Machine

F. I. Apeh, B. S. Yahaya, F. Achema, M. O. Fabiyi and E. S. Apeh
*Engineering Materials Research Department, Nigerian Building and Road Research Institute, KM 10 Idiroko Road, Ota, Ogun State, Nigeria*

***ABSTRACT :****The technological advancement of any nation have been influenced and uplifted by the extent to which it can usefully harness and convert its mineral and local resources into household products and as such, the need to design an implements for their production. Design analysis of a fabricated palm kernel shells grinding machine using locally sourced materials was carried out. The machine was designed and fabricated from locally available materials for grinding palm kernel shell and likely limestone as well as animal bones into small particle size of less 425µm or greater than. The grinding process was achieved by the use of hammers in the grinding chamber with a three phase 75hp motor as prime mover. The design analysis carried out on the palm kernel shells grinding machine showed that the machine has a grinding efficiency of 97.9%, grinding capacity of 625kg/hr., percentage recovery of the material (palm kernel shell) is 92.6% and fineness modulus of 0.39.*

***Keywords -*** *Design Analysis, Fine Particles, Grinding Efficiency, Grinding Machine, Palm Kernel Shell*

## I. INTRODUCTION

A grinding machine is a complex mechanism designed to break a solid material into smaller pieces or to the required sizes. There are different types of grinding machines for various materials processing. Historically, grinding mills or grinding machines were powered manually (mortar and pestle), or by using working animal (horse mill), wind (wind mill) or water (water mill), but in the recent time, it is been powered by A.C or D.C power supply. Grinding of solid matters occurs under mechanical forces that trench the structure by overcoming the interior bonding forces. After grinding, the state of the solid is changed; the grain size, the grain size disposition and of which the grain shape are also affected [1].

Palm kernel shells (PKS) are fibrous, tough and hard material that covers the palm nut after the removal of oil rich outer cover. It has been found that, the shell contains some chemical, physical and mechanical properties that make it very useful in some other areas of applications [2]. The ash generated from burning off palm kernel shells has been found to be a good binder when mixed with appropriate ratio to ordinary Portland cement [3]. Palm kernel shells are also used as bio-carbon in water treatment plant [4]. A typical palm kernel shell has the following chemical and physical properties: the chemical properties are; Calcium Oxide (CaO)-8.786%, Silicon Oxide ($SiO_2$)- 54.81%, Potassium Oxide ($K_2O$)- 6.254%, Magnesium Oxide (MgO)- 6.108%, Iron oxide ($Fe_2O_3$) - 0.362%, Alumina ($Al_2O_3$)-11.40% and the physical properties are; moisture content - 6.11%, ash content - 8.6%, bulk density{(wet and dry),- 7.40kg/$m^3$and - 9.24kg/$m^3$ respectively}, porosity {(wet and dry) - 28% and - 65% respectively}[5,6]. Palm kernel shell has been found to have a calorific value of 5.2MWh/MT [7]. The desire to design and fabricate PKS grinding machine was borne out of the needs to develop indigenous technological innovation for processing of semi raw materials. The PKS grinding machine was designed for processing or grinding palm kernel shells into the required particle size. The main aim of this work is to grind palm kernel shells so that it can be mixed with clay (powder) during nodulization process for the production of pozzolana cement. During the process, the PKS serves as fuel and subsequently became binder after ball milling. The machine is of hammer mill type of which the hammers are mounted on a shaft in the chamber for the milling operation. The hammers revolve at high speed in the chamber and as the hummers hit the dry shells repeatedly, the materials are reduced to the required particle size. The machine is incorporated with an adjustable separator for possible regulation of the PKS particle size during the operation. It is powered with 75hp electric motor of 1,440 rpm. The design and fabrication of this machine tend to solve and encourage the use of locally available raw materials and boost capacity building in the area of machine construction for their application in relevant field.

## II. METHODOLOGY

### 2.1 Design Analysis

In carrying out the design, all the various components that require proper calculation were considered. Some of these component parts are: the shaft, belt length, hammer's shaft diameter, etc. The main shaft is a rotating component that operates within a cylinder or housing. The speed of the shaft is an important factor that determines the performance of the machine. The shaft speed is derived as shown below:

Let the velocity of belt = V m/s (1)

Let the velocity of belt at the point of contact with wheel = V m/s (2)

and the relationship between angular and linear velocity is V = πND [8] (3)

Since, the velocity is the same on the large pulley and small pulley, then equation (4) below can be derived,

$$V_1 = V_2 \tag{4}$$

$$\pi N_1 D_1 = \pi N_2 D_2$$

from here, it implies that,

$$\frac{D_1}{D_2} = \frac{N_2}{N_1}. \tag{5}$$

where, $N_1$ = revolution of the smaller pulley (rpm), $N_2$ = revolution of the larger pulley (rpm), $D_1$ = diameter of the small pulley (mm), $D_2$ = diameter of the large pulley (mm). The exact shaft speed is only obtained when there is no slip condition of the belt over the pulley. When slip and creep condition is present, the value of the rotational speed is reduced by 4% [9].

### 2.2 Determination of the Length of the Belt

The combination of pulleys and belts have two uses, that is, to increase or reduce speed or torque or to transfer power from one shaft to another. If the transfer of power is what is required, then two pulleys of the same diameter will do the work, but most of the time, the speed can be increased and or reduce the torque or vice versa. In this design, the speed of the system was increased while the torque reduces. This is done by using pulleys of different diameters. The belts were employed to transfer power through rotational motion from one shaft to another. The centre to centre distance between the large pulley and small pulley used in this design was measured and is equal to 117mm. The length of the desired belt is given by [10], equation (6)

$$L = 2C + 1.57(D_2 + d_1) + \frac{d_1 + D_2}{4C}. \tag{6}$$

where, L = length of the belt, mm, C = the centre to centre distance between large pulley and the small pulley, $d_1$ = diameter of the small pulley and $D_2$ = diameter of large pulley, mm.

**Table 1**: Dimensions of standard V-belts [11]

| **Types of belt** | **Power ranges [kw]** | **Minimum pitch diameter of pulley, D[mm]** | **Top width, b[mm]** | **Thickness, t[mm]** |
|---|---|---|---|---|
| **A** | 0.7-3.7 | 75 | 13 | 8 |
| **B** | 2-15 | 125 | 17 | 11 |
| **C** | 7.5-75 | 200 | 22 | 14 |
| **D** | 20-150 | 355 | 32 | 19 |
| **E** | 30-350 | 500 | 38 | 23 |

\

### 2.3 Determination of the Belt Contact Angle, (β)

Belt drives depend on friction between itself and the pulley. Excessive friction leads to wastes of energy and rapid wears of the belt [12]. There are some factors that affect belt friction, which include tension, contact angle and the materials used for the production of the belt and pulley. In other to minimize excessive friction in any machine, a smaller belt contact angle is required, because the smaller the belt contact angle the lower the heat generated between the pulleys and the belts. Belt contact angle is given by [12], equation (7):

$$\beta = \sin^{-1}\frac{D-d}{C}. \tag{7}$$

where, D = diameter of the large pulley, mm, d = diameter of the small pulley, mm, and **C** = the centre to centre distance between large pulley and the small pulley, mm

The angles of wrap for the pulleys which is used to determine the governing pulley is given by [8], equation (8) and equation (9):

$$\alpha_1 = 180 - \sin^{-1}\left(\frac{D-r}{C}\right). \tag{8}$$

$$\alpha_2 = 180 + \sin^{-1}\left(\frac{D-d}{C}\right). \tag{9}$$

where, $\alpha_1$ = angle of wrap for the smaller pulley, degree, $\alpha_2$ = angle of wrap for the larger pulley, degree.

## 2. 4 Determination of the Belt Tension

This is to determine how much load a belt can carry before it slips and this depends on a lot of factors, which have been discused earlier. The most important among them is the initial tension i.e., the force pulling the pulley(s) toward each other when at rest. When the belt is slack , little initial tension will result in slipping of the belt, and when it is too tight, it will lead to unnecessarily stresses and subsequently wearing the bearings. The belt tension is calculated [13], using equation (10):

$$T_2 = \frac{(T_1 - mv^2)}{exp\left[\frac{\mu\alpha}{\sin\frac{\theta}{2}}\right]}. \tag{10}$$

where, $T_1$ = the tension in the tight side of the belt ($T_1$ = SA), $T_2$ = the tension in the slack side of the belt, S = the maximum permissible belt stress, A = area of belt, m = mass per unit length of belt, v = linear velocity of the belt ($mv^2$ = centrifugal force acting on the belt), μ= is constant=0.25, $\alpha$ = angle of wrap, degree., $\theta = 40^o$.

## 2.5 Determination of the Power been Transmitted to the Shaft, Torque and Elastic Creep

Power transmission is the movement of energy from its place of generation to a location where it is applied to perform a useful work. While Torque is a measure of how much force acting on an object causes that object to rotate. The power transmitted to the shaft is determined by considering the tension in the slack and tight side of the belt and the velocity of the belt.

Let $T_1$ be the tension in the tight side, $T_2$ the tension in the slack side and V, the velocity of the belt in m/s. Power transmission to the shaft is derived by [8], equation (11) which involves mechanical power and is the product of force and velocity [8],

so,

$$P = F \times v \tag{11}$$

where, P= is the power, F=is the force, v= is the velocity and is equal to πND, N = the number of revolution per minute, D=the diameter the of pulley.

In the design, there is a force pulling in opposition to the other, hence, the net power transmitted is:

$$P = (T_1 - T_2)v \tag{12}$$

$$P = \pi ND(T_1 - T_2) \tag{13}$$

The presence of friction between pulley and belt causes differential tension in the belt. This differential tension causes the belt to elongate or contract and create a relative motion between the belt and the pulley surface. This relative motion between the belt and the pulley surface is created due to the phenomena known as elastic creep. The belt always has an initial tension when installed over the pulleys. This initial tension is the same throughout the belt length when there is no motion. During rotation of the drive, tight side tension is higher than the initial tension and slack side tension is lower than the initial tension. When the belt enters the driving pulley it is elongated and while it leaves the environment it contracts. The average belt velocity on the driving pulley is slightly lower than the speed of the pulley surface [8].

The equations below express the magnitude of the initial tension in the belt [8]:

$$\textbf{Tight side elogation} \propto (T_1 - T_i) \tag{14}$$

$$\textbf{Slack side contraction} \propto (T_i - T_2) \tag{15}$$

where, $T_i$ is the initial belt tension.

Since belt length remain the same i.e., elongation is the same as the contraction,

$$T_i = \frac{T_1 + T_2}{2} \tag{16}$$

Torque (τ) at the main shaft is calculated by considering the tension in the tight side of the belt ($T_1$), as well as tension in the slack side of the belt ($T_2$) and the radius of the main shaft (R) [8], equation(17):

$$\tau = (T_1 - T_2)R \tag{17}$$

The force exerted on the main shaft of the machine is determined by calculating the weight of individual hammers. The weight ($W_h$) of each hammer is calculated by the relation below:

$$W_h = m_h g \tag{18}$$

where, $m_h$ is the mass of one hammer (kg), $g$ is constant, that is, acceleration due to gravity ($10m/s^2$). The total force ($F_t$) to be exerted on the main shaft is calculated by multiplying the weight of each hammer ($W_h$) by the total number of hammers weight, equation (19):

$$F_t = W_\Sigma x\ g = 284.2N \tag{19}$$

where, $W_\Sigma$ = total weight of the hammers, Kg, g = acceleration due to gravity ($10m/s^2$).

### 2.6 Determination of Centrifugal Forces on the Hammers

The centrifugal force ($F_c$) that may be exerted by the hammers on the main shaft of the machine is determined by considering the mass (m) of the main shaft, radius of the main shaft (r) and the velocity (v) of the main shaft, equation (20):

$$F_c = \frac{mv}{r} \tag{20}$$

### 2.7 Determination of the Hammer Shaft Diameter

In order to come up with the shaft diameter the bending moment needed to be considered. The bending moment ($m_{b(max)}$) on the shaft is given by [14], equation (21):

$$m_{b(max)} = \frac{wl^2}{8} \tag{21}$$

Since the bending moment ($m_b$) of a beam is a measure of the strength of such beam, it hence depends upon the loading and resultant reactions (I/y$\mu a\theta$) [14], the allowable stress ($\sigma_s$) of a beam is equal to:

$$\sigma_{s(allowable)} = \frac{m_b Y_{max}}{I} \tag{22}$$

Z = section modulus of the beam = $\frac{I}{Y_{max}}$,

therefore,

$$\sigma_{s(allowable)} = \frac{m_b}{Z} \tag{23}$$

where $Y_{max}$= distance from neutral axis to outer fibers, I = moment of inertia, Z = Section modulus, $m_b$= bending moment. For a solid round bar I and Z is given as [12]:

$$I = \frac{\pi d^4}{64} \tag{24}$$

and

$$Z = \frac{\pi d^3}{32} \tag{25}$$

The schematic diagram of the PKS grinding machine is as shown in Figure 1 below.

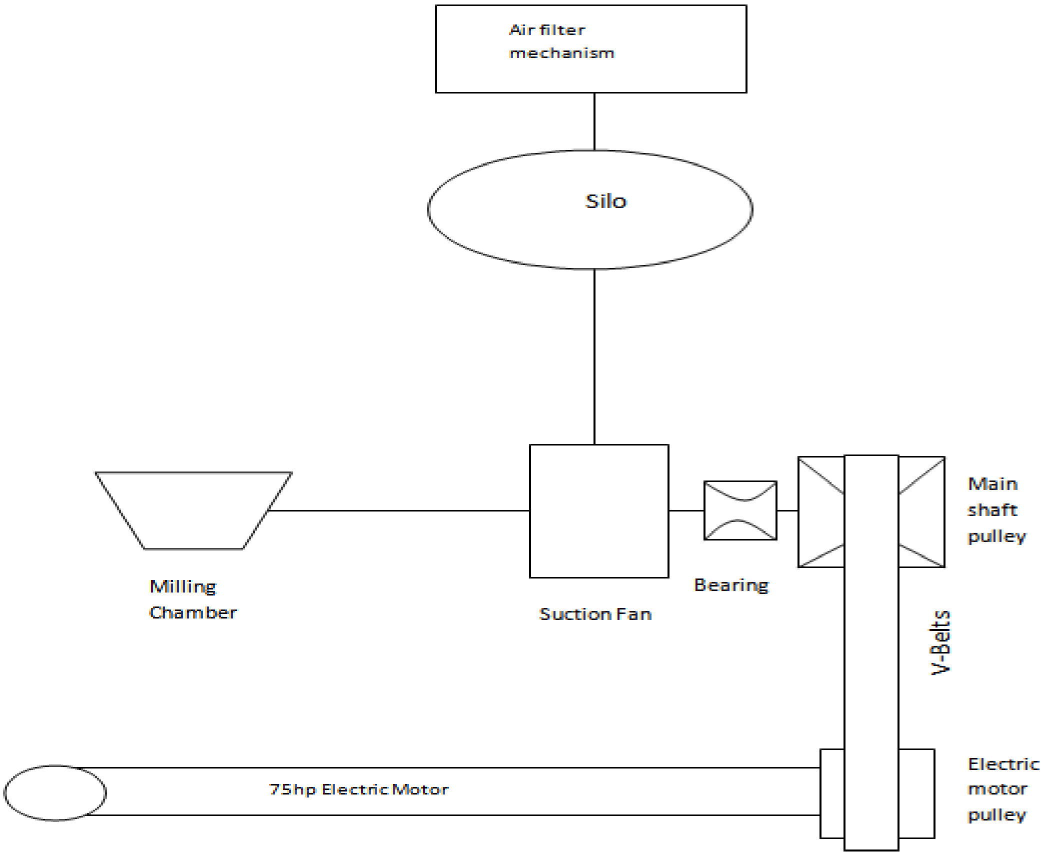


**Figure 1:** Schematic Diagram of the Fabricated PKS Grinding Machine

### 2.8 Determination of the main Shaft Diameter

The American Society of Mechanical Engineers (ASME) code equation for a solid shaft having little or no axial loading is [10]:

$$d^3 = \frac{16}{\pi \sigma_s}\sqrt{(k_b m_b)^2 + (k_t m_t)^2} \quad (26)$$

where, d = diameter of shaft, $\sigma_s$ = allowable stress (55MN/m$^2$ for shaft without keyway and 40MN/m$^2$ for shaft with keyway), $K_b$ = factor for gradually applied load = 1.5, $K_t$ = factor for suddenly applied load = 1.5. The result of the calculations are tabulated in Table 2

### 2.9 Construction Details of the Major Parts

***Main Shaft:*** A 100 mm diameter x 480 mm length rod of tool steel was used for the shaft. The shaft was faced and center drilled which was stepped turned to 90 and 80 mm at the hammer side and 90mm, 80mm and 70mm at the suction fan side. The keyway was milled out using milling machine.

***Beater Shaft:*** 15 mm diameter rod was cut, faced and turned to 12 mm diameter. The length of the shaft used was 70 mm.

***Hammer:*** 20 numbers of spring steel hammers were cut into 280mm by 108mm. A hole of 40 mm was drilled at the bottom of each hammer, using twist drill to enable it fit into the hammer shaft.

***Hopper:*** It is pyramidal in shape and it was made from a mild steel sheet of 1.5mm thick plate. It was dimensioned 204 x 204 mm top opening, 50 x 50 mm base opening and height 240 mm. The plate was marked and cut to sizes and then welded together using arc welding.

**Grinding Chamber:** A 10mm thick mild steel cylindrical drum of 1000mm by 800mm was cut into two of equal halves. The base layer of the cylindrical drum was lined with 10mm thick mild steel sheet while 8mm thick mild steel sheet was used to lined the upper layer of the chamber. Hinges and bolts brackets were welded to the edge of the upper and base layer of the cylinder drum to form the grinding chamber. The chamber houses the hammers, hammer shaft, suction fan, separator, and the main shaft.

### 2.10 Testing

Testing is a vital step in the process of machine development after the design and construction and this is necessary in order to:

- determine the performance of the machine;
- expose defect and area of possible improvement; and
- appreciate the level of success in the research carry out.

The resultant of the above is to determine the workability and efficiency of the machine.

### 2.11 Testing of Palm Kernel Shell Grinding Machine

In carrying out the test, the machine was on and allowed to operate for few minutes before loading in the dry PKS (50kg) through the hopper. The grinding time was noted and recorded. This operation was repeated for three times and the average was used for the calculation. After the testing, the machine was used for continuous loading and the materials grinded and sucked into the silos prior to discharging.

## III. RESULTS AND DISCUSSION

### 3.1 Results

The result of the calculations made and performance analysis carried out on the machine is shown in Table 2 and Table 3 below.

**Table 2**: Calculated Parameters

| Parameters | Symbol | Value | Unit |
|---|---|---|---|
| Shaft Speed | $N_2$ | 1800 | Rpm |
| Length of Belt | L | 800 | Mm |
| Belt Velocity | $V_b$ | 15.07 | m/s |
| Belt Contact Angle | B | 19.99 | Degree |
| Angle of wrap for smaller pulley | $\alpha_1$ | 160.01 | Degree |
| Angle of wrap for larger pulley | $\alpha_2$ | 199.99 | Degree |
| Tension in the slack side of belt | $T_2$ | 1183.34 | N |
| Tension in the tight side of belt | $T_1$ | 4895.05 | N |
| Initial Tension of the Belt | $T_i$ | 3039.20 | N |
| Torque at the hammer shaft | $\tau_h$ | 296.88 | Nm |

| | | | |
|---|---|---|---|
| Torque at the main shaft | $\tau_m$ | 371.17 | Nm |
| Power transmitted to the shaft | P | 55935.47 | W |
| Weight of hammer | $W_h$ | 14.21 | N |
| Centrifugal force exerted by the hammer | C.F | 3710.71 | N |
| Diameter of hammer shaft | d | 12 | mm |
| Diameter of main shaft | D | 200 | mm |

**Table 3:** Performance Result of the PKS Machine

| Test | Quantity (Kg) | Obtained Product (Kg) | Loss | Percentage Recovery (%) | Percentage Loss (%) |
|---|---|---|---|---|---|
| **1** | 50 | 48.25 | 1.75 | 96.5 | 3.5 |
| **2** | 50 | 47.70 | 2.30 | 95.4 | 4.6 |
| **3** | 50 | 48.30 | 1.70 | 96.6 | 3.4 |

$$\text{Average Percentage Recovery} = \frac{96.5+95.4+96.6}{3} = 96.2\ \% \qquad (27)$$

### 3.2 Discussions

In this project, a PKS grinding machine was design and fabricated with an adjustable separator for easy control of grain size. The test results show that, the fabricated PKS grinding machine has satisfactory performance in productivity, the grinded materials has low product temperature, which is very good for feed quality.

To select the right type of belt after the required belt length has been determined; power range, minimum pitch diameter, top width and thickness of the pulley were considered. V-belts were considered based on the calculation and that, they transfer torque effectively notwithstanding that they loose a bit of speed as the belt stretches under load. From Table 1, a standard V-belt of designation C115 was selected based on the power range.

From Table 2, it was observed that the value of $T_1$ is greater than that of $T_2$ which shows that the slack side of the belt is in the upper side and the tight side of the belt is in the lower side, which gives rise to the low value of the belt contact angle as required. Shaft size is dictated by torque but changes in horsepower and speed (RPM) affect torque [15] and this explains the variation between the value of the main shaft and the hammer shaft with their respective torque values as shown in Table 2. From the calculation in equations (8 and 9), it was discovered that the figure obtained for the small pulley is smaller, hence it governs the drive. From the expression in equation (16), increase in initial tension will lead to power transmission increase. If initial tension is gradually increased then $\mathbf{T_1}$ will also increase and at the same time $\mathbf{T_2}$ will decrease. Thus, if it happens that $\mathbf{T_2}$ is equal to zero, then $\mathbf{T_1 = 2T_i}$ **(16)** and from there maximum power transmission will be achieved [8].

It has been observed from the result of the tests that, the grinding efficiency of the machine was found to be 97.7% and production capacity was 625 Kg/hr of the dry PKS. It is clear from the grinding capacity and efficiency as enumerated above that, the performance of the machine is excellent. The average percentage recovery was 96.2%. The loss in the materials grinded as obtained from the original quantity fed into the machine was due to the sticking of the powdery materials to the wall of the grinding chamber and escape of powdery materials through some tiny holes along the line of discharge during production.

## IV. CONCLUSION

The design and fabrication of palm kernel shell grinding machine was based on the need to develop indigenous technology for processing of raw materials. Detailed calculations made and the use of locally available raw materials for the fabrication of the machine has significant technological benefit. From the design consideration and analysis; reliability, safety, serviceability and cost of construction were given due consideration. From the design analysis on the fabricated palm kernel shell grinding machine the following can be established:

i) Grinding Efficiency = 97.7%;
ii) Grinding Capacity = 625 Kg/hr; and
iii) Percentage Recovery = 96.2%.

The adjustable separator screen attached to the suction outlet gives room for sizing of the various grain sizes needed for different production purposes and based on the above, the design analysis was successful carried out.

## REFERENCES


[1] Http://en.wikipedia.org/wiki/Crusher, accessed on the 14/4/ 2014.

[2] Omange G. N., Palm kernel shells as road building materials, *Technical Transactions of the Nigerian Society of Engineers*, 36(1), pp. 17-25. 2001

[3] Uviasah M. O., *Properties of Palm kernel shells and Fibre as aggregates for making concrete*, Unpublished Bachelor of Engineering Thesis, Department of Civil Engineering, University of Benin, Benin, Nigeria. 1976

[4] Neville A. M., Properties of concrete (Pearson Education, Asia Pte ltd, Edingburg, Scotland, 1995) pp. 108-176.

[5] Akpe, E., *Characteristics Strength of Concrete using Palm kernel shells as light weight aggregate*, Unpublished Technical Report, Department of Civil Engineering, Edo State University, Ekpoma, Nigeria. 1997

[6] Festus A. Olutoge, Habeeb A. Quadri, and Oladipupo S. Olafusi, Investigation of the Strength Properties of Palm Kernel Shell Ash Concrete, *ETASR - Engineering, Technology & Applied Science Research Vol. 2, No. 6*, 2012, pp315-319.

[7] Dagwa,I. M, and Ibhadode, A. O, Some physical and Mechanical properties of palm kernel shell (PKS), *Botswana Journal of Technology, Vol. 17, No. 2*, 2008, pp 10-16.

[8] Khurmi, R.S. and Gupta J. K., *Text book on Machine Design* (Eurasia Publishing House, New Delhi. 2008)

[9] Spolt, M. F., *Design of Machines Element* (6th ed. Prentice Hall, New Delhi, India. 1988)

[10] John, H., and Stephens, R. C., *Mechanic of Machines* (4th ed., 24, Edward, London, England, 1984)

[11] Khurmi, R. S. and Gupta, J. K., Shaft, V-belt and Rope Drives: *A Textbook of Machine Design*. 13thEdition. (S. Chand and Co. Ltd., New Delhi, 2004) pp: 456-498, 657-659.

[12] Jimoh, M. O. and Olukunle, O. J., Design of an effective automated machine for quality palm kernel production, *IOSR Journal of Mechanical and Civil Engineering (IOSR-JMCE) e-ISSN: 2278-1684 Volume 6, Issue 1*, 2013, PP 89-97.

[13] Maitra, G. M., and Prasad, L.V., *Handbook of Mechanical Design* (McGraw Hill, New Delhi, India, 1985) pp. 89-108.

[14] Ryder, G. H, *Strength of Material* (3rd ed. Catalogue 300E/EB 666, SKF General Catalogue Macmillan, New York, USA. 1969)

[15] http://www.pumpsandsystems.com/topics/motors/relationship-torque-and-shaft-size-0#sthash.5us0UciZ.dpuf, accessed on the 13/3/ 2015.